

Partitioning of the Leaf CO₂ Exchange into Components Using CO₂ Exchange and Fluorescence Measurements¹

Agu Laisk* and Astrid Sumberg

Institute of Molecular and Cell Biology, Tartu University, 181 Riia Street, Tartu, Estonia EE2400

Photorespiration was calculated from chlorophyll fluorescence and ribulose-1,5-bisphosphate carboxylase/oxygenase (Rubisco) kinetics and compared with CO₂ evolution rate in the light, measured by three gas-exchange methods in mature sunflower (*Helianthus annuus* L.) leaves. The gas-exchange methods were (a) postillumination CO₂ burst at unchanged CO₂ concentration, (b) postillumination CO₂ burst with simultaneous transfer into CO₂-free air, and (c) extrapolation of the CO₂ uptake to zero CO₂ concentration at Rubisco active sites. The steady-state CO₂ compensation point was proportional to O₂ concentration, revealing the Rubisco specificity coefficient (K_{sp}) of 86. Electron transport rate (ETR) was calculated from fluorescence, and photorespiration rate was calculated from ETR using CO₂ and O₂ concentrations, K_{sp} , and diffusion resistances. The values of the best-fit mesophyll diffusion resistance for CO₂ ranged between 0.3 and 0.8 s cm⁻¹. Comparison of the gas-exchange and fluorescence data showed that only ribulose-1,5-bisphosphate (RuBP) carboxylation and photorespiratory CO₂ evolution were present at limiting CO₂ concentrations. Carboxylation of a substrate other than RuBP, in addition to RuBP carboxylation, was detected at high CO₂ concentrations. A simultaneous decarboxylation process not related to RuBP oxygenation was also detected at high CO₂ concentrations in the light. We propose that these processes reflect carboxylation of phosphoenolpyruvate, formed from phosphoglyceric acid and the subsequent decarboxylation of malate.

Photorespiration of C₃ plants was discovered by Decker (1955) from measurements of a postillumination CO₂ burst. Photorespiration can also be observed as CO₂ evolution after rapid transfer of the leaf into a CO₂-free gas (Forrester et al., 1966). Since the CO₂ concentration at which photosynthesis and photorespiration equilibrate was found to be proportional to O₂ concentration and independent of light intensity, it was suggested that CO₂ and O₂ compete for the primary acceptor RuBP at the carboxylase/oxygenase sites (Laisk, 1970). This was proven with the partially purified enzyme (Ogren and Bowes, 1971) and at present it is generally accepted that photorespiration is a result of the functioning of the glycolate cycle (Hess and Tolbert, 1966; Kisaki and Tolbert, 1970; Lorimer, 1981).

Measurements of photorespiration are complicated because reassimilation of CO₂ obscures the true CO₂ evolution rate in the light. Reassimilation in leaf intercellular spaces can be accounted for by calculating the intercellular CO₂ concentra-

tion (Laisk and Oja, 1972). The postillumination photorespiratory CO₂ burst is also partially reassimilated by the assimilatory charge (Laisk et al., 1984; Laisk et al., 1987; Sharkey, 1988), which is closely equivalent to the pool of RuBP present in the leaf when illumination is interrupted. Calculations of reassimilation in the mesophyll cells are complicated, since the CO₂ transport resistance in the mesophyll cells is difficult to determine (Evans et al., 1986; von Caemmerer and Evans, 1991; Harley et al., 1992; Loreto et al., 1992). The mechanism based on the competition of CO₂ and O₂ at Rubisco has generally been found to fit the experimental data (Laisk, 1970; Laisk and Oja, 1972; Peterson, 1987, 1989; Cornic and Briantais, 1991). The range of CO₂ pressures applied in these measurements has usually been below 600 μ bars, which has left out the interesting range of depression of photorespiration by CO₂. At saturating CO₂ concentrations the CO₂ evolution in the light proceeds faster than predicted from the theory, and this CO₂ is evolved from freshly assimilated carbon pools. This has led to suggestions that the CO₂/O₂ competition mechanism of photorespiration is not adequate at high CO₂ concentrations (Bravdo and Calvin, 1979; Keerberg et al., 1983; Pärnik, 1985).

In this work we have used a fast-response gas-exchange system for the measurements of photorespiration over a wide range of CO₂ concentrations. Simultaneously, electron transport rates were determined from fluorescence measurements. This allowed a comparison of the rates of photorespiration obtained from gas exchange with those calculated from the electron transport rate. As a result we can distinguish four components of gas exchange in the light. We confirm that at high CO₂ concentrations photorespiration is suppressed, as predicted by the Rubisco kinetics. Instead, a carboxylation and a decarboxylation, not directly related to the photosynthetic electron transport, dominate at these CO₂ concentrations.

MATERIALS AND METHODS

Sunflower (*Helianthus annuus* L.) plants were grown in a growth chamber at a PFD of 46 nmol cm⁻² s⁻¹, 18/6 h day/

Abbreviations: $B(\text{CO}_2)$, postillumination CO₂ burst in the presence of a stated concentration of CO₂; $B(0)$, postillumination CO₂ burst in the absence of CO₂; C_c , chloroplast CO₂ concentration; ETR, electron transport rate; Γ , steady-state CO₂ compensation point; Γ^* , CO₂ photocompensation point; K_{sp} , Rubisco specificity coefficient; $P(\text{CO}_2)$, net CO₂ assimilation rate; PAD, photon absorption density; PFD, photon flux density; PGA, 3-phosphoglyceric acid; R_L , total respiration in the light; r_{md} , CO₂ transport resistance in mesophyll cells; RuBP, ribulose-1,5-bisphosphate.

¹ This work was supported by Estonian Science Foundation, grant 108, and International Science Foundation, grant LCS000.

* Corresponding author; fax 372-7-430365.

night cycle, air temperature 28/20°C day/night, RH 50 to 60% by day, on well-fertilized peat-soil mixture in 4-L pots. Attached upper, fully expanded leaves of 4-week-old plants were used.

The gas-exchange apparatus contained two open gas-flow systems (channels A and B) in which the gas composition could be adjusted separately (Oja, 1983; Laisk et al., 1984). An Infralyt 3 analyzer (Junkalor, Dresden, Germany) was used for the recording of CO₂ concentration at the end of channel A, and an LI-6262 analyzer (Li-Cor, Lincoln, NE) was used in channel B. Water vapor was recorded by psychrometers in each channel. Gas was dried to a constant humidity in small Peltier-cooled condensers before entering the CO₂ analyzers. During the measurements a part of the leaf was enclosed in a sandwich-type cuvette (4.4 × 4.4 × 0.3 cm³, gas flow rate 20 cm³ s⁻¹). For temperature stabilization the leaf blade was fixed with starch paste directly to the cuvette window, which was thermostated by water from the other side. Water temperature was 21.5°C, and leaf temperature was 22.2°C in the light. Gas exchange proceeded via the lower epidermis of the leaf only. As a result, the CO₂-limited gas-exchange rates were probably somewhat reduced. This did not influence the values of the CO₂ bursts nor the other results that were based on calculated chloroplast CO₂ concentration.

The leaf chamber could be connected with the gas flow of either channel A or channel B by a special stopcock, which made it possible to rapidly change the CO₂ concentration in the leaf chamber to the levels preadjusted in the channels. While the chamber was in channel A, channel B was circuited through an equivalent resistance so that the gas analyzer in channel B showed the reference line and that in channel A showed the leaf response and vice versa when the chamber was connected with channel B. The full response time of the system, determined mainly by gas flow: volume ratios, was 2 s for CO₂ with the LI-6262 in channel B. Channel A was used mainly for the preconditioning of the leaf to its steady state and channel B was used for the measurement of the fast leaf responses.

The CO₂ analyzers were calibrated by means of dynamic capillary gas mixers with 1% accuracy in the range from 0 to 2000 ppm CO₂ (Oja, 1983). C_c was calculated as outlined by Laisk (1977), taking into account the effect of water vapor counterflow for CO₂ diffusion in stomatal pores, the solubility of CO₂ in cell water, and CO₂ transport resistance in cells. Following the precedent laid down by Brown and Escombe (1900) and Laisk and Oja (1971, 1972), we express CO₂ as its concentration, not as partial pressure or mole fraction as suggested by Cowan (1977). Accordingly, the CO₂ and O₂ will be expressed in μM (nmol cm⁻³), rates (including photon flux rate) in nmol cm⁻² s⁻¹, and diffusion resistances in s cm⁻¹. These units are compatible with molar concentrations of metabolites and allow us to calculate the Rubisco specificity factor in vivo. The Bunsen solubility constants of 0.89 for CO₂ and 0.029 for O₂ at 22.2°C were applied. We still use mole fraction (ppm) to denote the CO₂ concentration at the inlet of the leaf chamber.

Three procedures for determining photorespiration were used: (a) postillumination CO₂ burst without changing the CO₂ concentration, (b) postillumination CO₂ burst with si-

multaneously changing to CO₂-free gas, and (c) initial CO₂ evolution into CO₂-free gas in the light, corrected for CO₂ reassimilation.

A special, six-branch fiber optic was designed for leaf illumination and optical measurements. Plastic fibers of 1 mm diameter (Toray polymer optical fiber, PF-series, from Laser Components, Gröbenzell/München, Germany) were arranged into a bundle of 45 × 45 mm², which was attached to the leaf cuvette. The free ends of the fibers were divided into branches; two were used for illumination by actinic light and saturation pulses and two for excitation and measurement of the Chl fluorescence. Chl fluorescence was measured by a PAM 101 fluorometer (H. Walz, Effeltrich, Germany) at two spots of 10 × 20 mm symmetrically placed over the leaf chamber, avoiding the midrib. A Schott KL 1500 light source was used for actinic illumination and a 1000-W DC xenon arc lamp, equipped with a cold mirror and a heat-reflecting filter, provided saturation flashes of 800 nmol cm⁻² s⁻¹, of 1 s duration. The electron transport rate was calculated as proposed by Genty et al. (1989):

$$ETR = \frac{F'_m - F}{F'_m} \times PAD \times 0.5 \quad (1)$$

where PAD was measured by the LI-190SB quantum sensor (Li-Cor) and multiplied for the leaf absorbance measured in an integrating sphere with the same actinic light and sensor F is steady-state fluorescence yield; and F'_m is fluorescence yield in saturation flashes. The assumption that 0.5 PAD was absorbed by PSII gave reasonably good coincidence between the fluorescence and gas-exchange data under nonphotorespiratory conditions.

RESULTS

Measuring Respiration in the Light by Transients of the CO₂ Exchange

Postillumination CO₂ burst is the simplest method for the measurement of photorespiration and is based on the consideration of the different decay kinetics of photosynthesis and photorespiration. Such a postillumination transient at normal atmospheric CO₂ and O₂ concentrations is shown in Figure 1 (curve 1). The CO₂ uptake approached zero after 5 s and the rate of CO₂ evolution peaked 13 s from darkening. From this recording it is evident that the maximum rate for the postillumination CO₂ burst $B(\text{CO}_2)$ (arrow) is a compromise between the postillumination CO₂ reassimilation in the first 10 s and a declining rate of photorespiration. In Figure 2 the same experiment was repeated with 2000 ppm CO₂, which would severely suppress photorespiration. There was no CO₂ burst and at 13 s from the transition to darkness the CO₂ evolution rate was still increasing.

Curve 2 in Figure 1 is the postillumination CO₂ burst after transition of the leaf into CO₂-free air of channel B simultaneously with darkening, $B(0)$. With this method we avoided the uptake of external CO₂ during the postillumination CO₂ burst (but not reassimilation of the photorespiratory CO₂). To bypass the big flux of dissolved CO₂, which evolved from the leaf during the first 2 s (Oja et al., 1986), the gas flow was not connected with the analyzer of channel B for 2 s

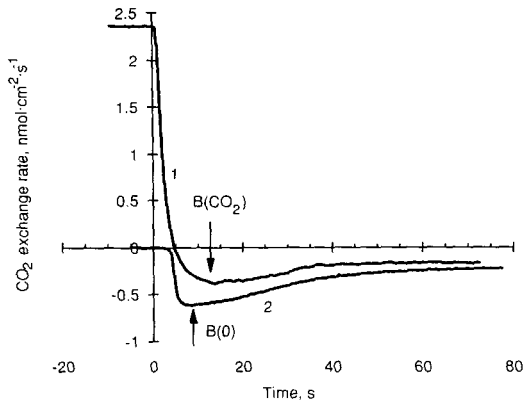


Figure 1. Postillumination transients in CO₂ exchange rates. Sunflower leaf was exposed at 300 ppm CO₂, 21% O₂, PAD of 120 nmol cm⁻² s⁻¹, in steady state. At time = 0 light was switched off (curve 1). In another, similar experiment CO₂ concentration was changed to 0 simultaneously with darkening by switching the leaf chamber from channel A to channel B (curve 2). Values of the postillumination CO₂ burst in the presence, $B(\text{CO}_2)$, and absence, $B(0)$, of CO₂ were read at arrows.

from the moment of the transition. As a result, the analyzer of channel B continued to record its baseline for the first 2 s in the dark, as seen from curve 2 in Figure 1.

In CO₂-free air the postillumination CO₂ burst, $B(0)$, was greater and the maximum occurred earlier than in the presence of CO₂. After 60 s the CO₂ evolution declined to a minimum and then increased again (not shown in Figs. 1 and 2). The difference between the two curves for the CO₂ bursts in Figure 1 shows that there was a small postillumination CO₂ uptake component in gas exchange that shifted the $B(\text{CO}_2)$ curve upward. In similar experiments started after photosynthesis with 2000 ppm CO₂ (Fig. 2, curve 2), the fast initial burst (until 7 s) was probably desolubilization of residual CO₂. However, the subsequent time course of the CO₂ evolution did not represent photorespiration but reflected another metabolic CO₂ evolution process with a relaxation

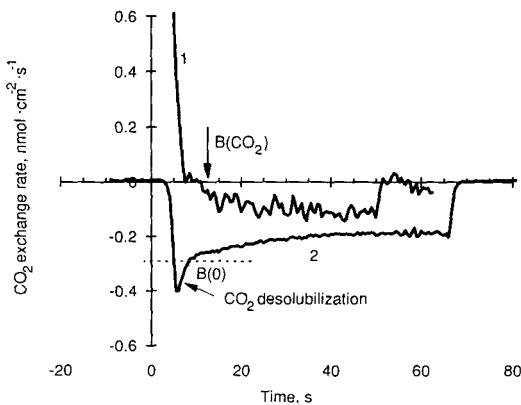


Figure 2. The same experiment as in Figure 1, except that the leaf was previously exposed in steady state to 2000 ppm CO₂. Recordings ended with switching the leaf chamber back to channel A to establish the reference line.

time of about 50 s. Because $B(\text{CO}_2)$ in the presence of 2000 ppm CO₂ was considerably higher than $B(0)$, the alternative carboxylation process was also present at this CO₂ concentration. Thus, the two postillumination CO₂ exchange curves, one recorded in the presence and the other in the absence of CO₂, reveal two simultaneous processes, a carboxylation and a decarboxylation, which have similar relaxation times of about 50 s.

The third gas-exchange method to measure photorespiration was the extrapolation of the linear part of the P versus C_c response curve to $C_c = 0$. This method has been used primarily starting from limiting CO₂ concentrations. When used from saturating CO₂ concentrations, fast recording is necessary to see the initial photorespiration rate before it increases at low CO₂ levels in the light. Two recordings made starting from 2000 ppm CO₂, one to 100 and the other to 0 ppm, are shown in Figure 3. Gas was flushed out during 2 s after the transition, as in the case of curve 2 in Figure 2. The slow changes in the CO₂ exchange were extrapolated to the beginning of the recordings, disregarding the initial peak of CO₂ desolubilization. The values obtained (A and B) were assumed to correspond to the previous CO₂ evolution at 2000 ppm. In Figure 4 the points A and B are plotted against the C_c values, calculated for the same initial rates (curve 4). Extrapolation of this plot to $C_c = 0$ represents the sum of all CO₂ evolution processes in the light at 2000 ppm CO₂, R_L . Figure 4 also shows other, similar P versus C_c plots from transients starting from 0, 100, and 300 ppm CO₂ (curves 1–3). It must be emphasized that the CO₂ compensation points obtained by interpolation between the two transient measurements are apparent, representing a varying equilibrium between rapidly increasing photosynthesis and slowly increasing photorespiration. The transient from 0 to 100 ppm may also be influenced by the partial deactivation of Rubisco.

Γ was found from the plot of the steady-state CO₂ exchange rates (filled squares in Fig. 4). The values of Γ were found from similar experiments at 1.1, 10, and 50% O₂ and plotted against the dissolved O₂ concentration (Fig. 5). The

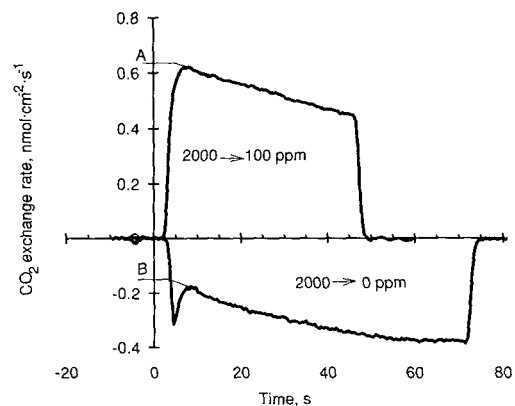


Figure 3. Transients in CO₂ exchange rate after changing CO₂ concentration in the light. The leaf was exposed at 2000 ppm CO₂, 21% O₂, in steady state. At time = 0 CO₂ concentration was changed to 100 ppm or to 0. The gas-exchange rate was extrapolated to the beginning of the transient disregarding the CO₂ desolubilization peak (A and B).

proportionality of Γ with O_2 concentration (Forrester et al., 1966; Laisk, 1977) was confirmed with great accuracy. The straight line in Figure 5 extrapolates very close to the origin of coordinates. This indicates that primarily photorespiratory CO_2 evolution was present in the light at Γ in mature sunflower leaves, with very little "dark" respiration. In a younger leaf this plot showed a small residual respiration, which did not disappear with photorespiration when O_2 approached zero. According to Laisk (1970) and Farquhar et al. (1980) the slope of this line is characteristic for the CO_2/O_2 specificity of Rubisco in vivo, $K_{sp} = 0.5[O_2]/\Gamma = 86$. In the younger leaf $K_{sp} = 92$. The value of $K_{sp} = 86$ was used in the analysis of the fluorescence data with the aim of finding the photorespiratory rate in an independent way.

The Influence of CO_2 Concentration on Respiration in the Light

Measurements similar to those in Figures 1 to 4 were carried out at different CO_2 and O_2 concentrations. Figure 6 shows the CO_2 dependencies of $P(CO_2)$, $B(CO_2)$, $B(0)$, and R_L , as revealed from the extrapolation of the P versus C_c plot. At 1.1% O_2 , RuBP oxygenation and, correspondingly, photorespiration were very low. The difference between the two CO_2 burst measurements, $B(CO_2)$ and $B(0)$, remained, but $B(CO_2)$ showed slightly positive values (it was always measured 13 s after the darkening). This result indicates that a postillumination CO_2 uptake process and not suppression of respiration at higher CO_2 levels was the cause of the difference between $B(CO_2)$ and $B(0)$. The maximum of $B(CO_2)$ at low CO_2 concentrations may be an artifact caused by lasting RuBP carboxylation.

In 21% O_2 , ETR was maximal at C_c values around 5 to 8 μM which are typical for leaves with open stomata under normal atmospheric conditions. It declines toward lower CO_2 concentrations because of the lack of sufficient electron ac-

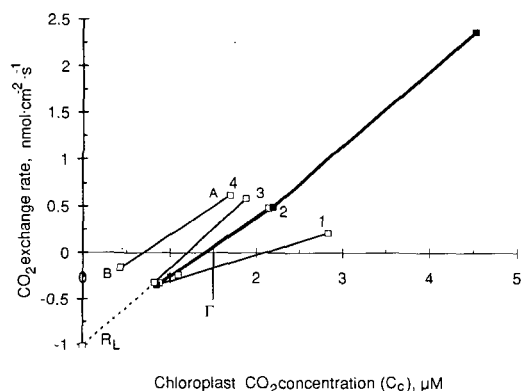


Figure 4. Determining CO_2 evolution in the light, R_L , by extrapolation of the P versus C_c curve to $C_c = 0$. Data points A and B from Figure 3 are plotted against calculated C_c (line 4). Other, similar transitions are from 0 ppm (steady state) to 100 ppm (line 1) from 100 ppm (steady state) to 0 ppm (line 2), and from 300 ppm (steady state) to 100 ppm and 0 ppm (line 3, extrapolation to $C_c = 0$ to find R_L is shown for this line). Filled squares represent the steady-state CO_2 curve used to find Γ at 21% O_2 .

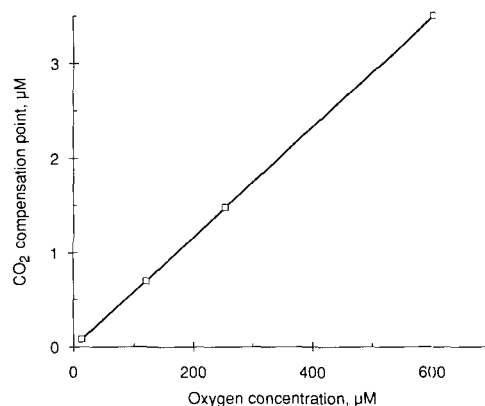


Figure 5. Dependence of Γ on the O_2 concentration in liquid phase of mesophyll cells.

ceptor and also toward higher CO_2 concentrations due to the inhibition of photorespiration by CO_2 . At Γ (the situation that occurs with closed stomata when no net CO_2 fixation is possible) ETR was reduced by only half. It was maintained so high due to the simultaneous turnover of CO_2 by the carbon reduction and glycolate cycles. Similar measurements done at 10 and 50% O_2 with the same leaf showed that the maximum ETR occurred at 21% O_2 .

The theory of photorespiration predicts a certain ratio of oxygenation and carboxylation (V_o/V_c) at any given $[O_2]/[CO_2]$ ratio (Farquhar and von Caemmerer, 1982):

$$\frac{V_o}{V_c} = \frac{V_{o\max}}{K_{mo}} \times \frac{K_{mc}}{V_{c\max}} \times \frac{[O_2]}{[CO_2]} = \frac{1}{K_{sp}} \times \frac{[O_2]}{[CO_2]} \quad (2)$$

where

$$\frac{V_{o\max}}{K_{mo}} \times \frac{K_{mc}}{V_{c\max}} = \frac{1}{K_{sp}} \quad (3)$$

Denoting the true photosynthetic rate $F = V_c$ and the photorespiration rate $R_p = 0.5V_o$, we have

$$\frac{F}{R_p} = 2 \times K_{sp} \times \frac{[CO_2]}{[O_2]} \quad (4)$$

Replacing the CO_2 fluxes by the corresponding electron flow rates, denoted here as J , we have

$$J_F = 4 \times F \quad (5)$$

and

$$J_{RP} = 8 \times R_p \quad (6)$$

which yields

$$\frac{J_F}{J_{RP}} = K_{sp} \times \frac{[CO_2]}{[O_2]} \quad (7)$$

On the other hand,

$$J_F + J_{RP} = J \quad (8)$$

Equations 7 and 8 form a system for the two unknowns J_F

and J_{Rp} from which

$$J_F = J \times \frac{K_{sp} \times C_c / [O_2]}{1 + K_{sp} \times C_c / [O_2]} \quad (9)$$

and

$$J_{Rp} = J \times \frac{1}{1 + K_{sp} \times C_c / [O_2]} \quad (10)$$

where C_c is substituted for $[CO_2]$ at the carboxylation sites. The corresponding CO₂ fluxes are

$$F = \frac{J}{4} \times \frac{K_{sp} \times C_c / [O_2]}{1 + K_{sp} \times C_c / [O_2]} \quad (11)$$

$$R_p = \frac{J}{8} \times \frac{1}{1 + K_{sp} \times C_c / [O_2]} \quad (12)$$

and the CO₂ exchange rate is

$$P = F - R_p = \frac{J}{4} \times \frac{K_{sp} \times C_c / [O_2] - 0.5}{1 + K_{sp} \times C_c / [O_2]} \quad (13)$$

On the other hand,

$$C_c = B \times C_a - P \times (B \times r_g + r_{md}) \quad (14)$$

Substituting C_c from Equation 14 into Equation 13 yields a quadratic equation

$$P = \frac{-b + \sqrt{(b^2 - 4ac)}}{2a} \quad (15)$$

where

$$a = -4 \times K_{sp} \times r / [O_2]$$

$$b = 4 \times (1 + K_{sp} \times B \times C_a / [O_2]) + J \times K_{sp} \times r / [O_2]$$

$$c = J \times (0.5 - K_{sp} \times B \times C_c / [O_2])$$

$$r = B \times r_g + r_{md}$$

In these equations B is the CO₂ solubility in water, C_a is ambient CO₂ concentration, r_g is diffusion resistance in the gas phase, and r_{md} is the CO₂ transport resistance in the liquid phase of mesophyll cells.

Equation 15 makes it possible to calculate the CO₂ exchange rate P from fluorescence data when diffusion resistances are known. The value of r_{md} was varied to find the best fit between the calculated and measured gas-exchange curves, as suggested by Harley et al. (1992). Once P was calculated, C_c was found from Equation 14 and substituted

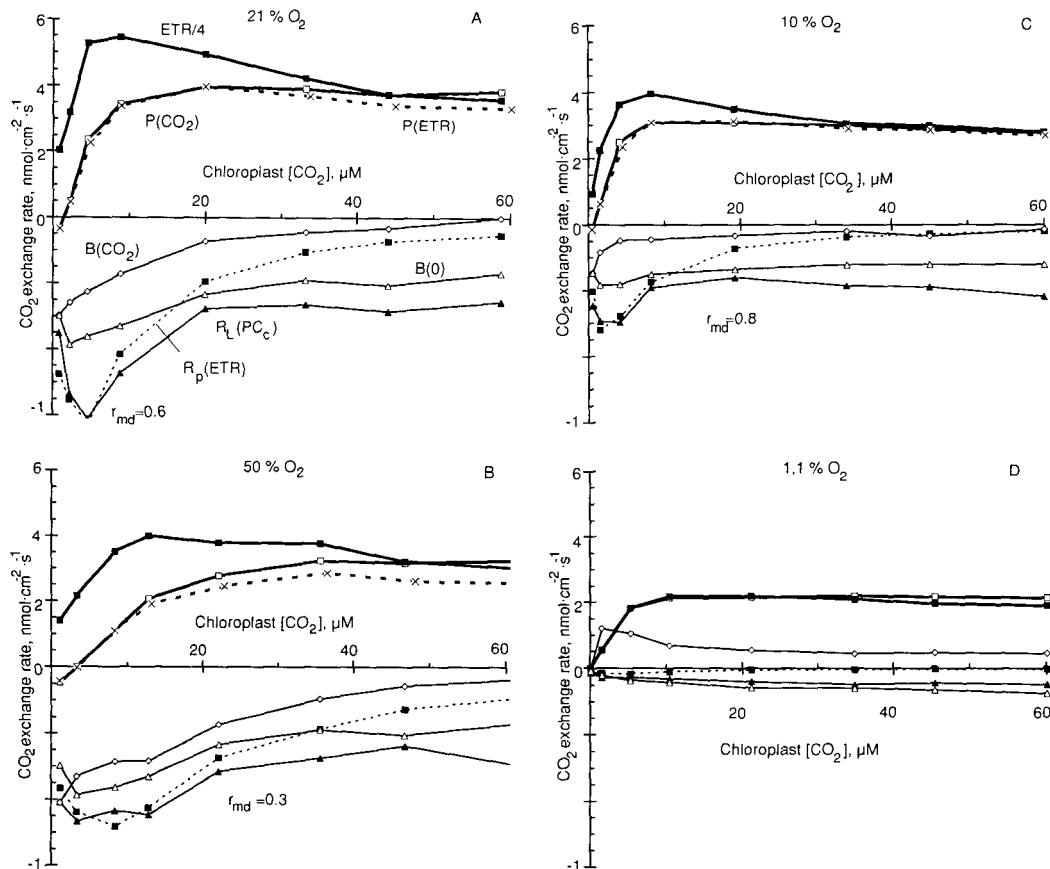


Figure 6. CO₂ dependencies of the measured $P(CO_2)$ (empty squares and thick line), $ETR/4$ (filled squares and thick line), $B(CO_2)$ (empty diamonds), $B(0)$ (empty triangles), and CO₂ evolution in the mesophyll cells in the light, $R_l(PC_c)$ (filled triangles). Dotted lines represent the rates calculated from ETR , the CO₂ exchange rate $P(ETR)$ (crosses), and photorespiration rate $R_p(ETR)$ (filled squares). Notice that the scales are stretched $\times 6$ for all CO₂ burst and respiration curves, but not for P below zero. A, 21% O₂; B, 50% O₂; C, 10% O₂; D, 1.1% O₂.

into Equations 11 and 12 to find the carboxylation and photorespiratory rates separately.

The thick dotted line and crosses in Figure 6 were calculated from Equation 15. Coincidence between the measured and calculated values for CO₂ net exchange is good at low CO₂ concentrations. At high CO₂ concentrations the measured gas-exchange rate tends to be greater than predicted. This shift is greater than experimental error and is present at all O₂ concentrations, pointing to a carboxylation that is not coupled to electron transport. The dotted line and filled squares in Figure 6 were calculated from Equation 12. The value of r_{md} was varied until the best fit between the fluorescence and gas-exchange measurements was obtained at the maximum of photorespiration. The values of the best-fit r_{md} ranged between 0.3 and 0.8 s cm⁻¹ for the same leaf at different O₂ concentrations.

DISCUSSION

In this work we measured CO₂ evolution in the light and electron transport rate in a wider range of CO₂ concentrations than previously reported (Peterson, 1989; Cornic and Briantais, 1991; Loreto et al., 1992). The fastest electron transport occurs around normal atmospheric CO₂ and O₂ levels, when both carboxylation and oxygenation of RuBP contribute the most. In the range of CO₂ saturation, *ETR* declines due to the outcompetition of O₂ by CO₂ at the Rubisco sites. The extent of this decline depends on the capacity of the leaf to activate starch synthesis (Sharkey and Vassey, 1989; Eichelmann and Laisk, 1994). Higher resistance to electron transport at saturating CO₂ has also been observed from the measurements of P700 redox state (Weis and Lechtenberg, 1989; Lechtenberg et al., 1990; Laisk et al., 1992). The decline of the net CO₂ assimilation rate with increasing CO₂ has been reported before (Woo and Wong, 1983), but the reasons for this phenomenon are obscure. One possibility is that Pi is being trapped in hexosephosphates and is no longer available for phosphorylation (Sharkey and Vassey, 1989; Eichelmann and Laisk, 1994).

This work shows that the best ¹²CO₂ gas-exchange method to estimate photorespiration rate is the extrapolation of the *P*(CO₂) versus *C_c* plot to *C_c* = 0, but it gives satisfactory results only at limiting CO₂ concentrations and requires knowledge of r_{md} . The values of the best-fit r_{md} ranged between 0.3 and 0.8 s cm⁻¹, which corresponds to the conductance of 0.52 to 1.04 μmol m⁻² s⁻¹ bar⁻¹. These values of CO₂ transport conductance in the mesophyll of sunflower-leaves extend the range of conductances obtained by Loreto et al. (1992), which ranged from 0.113 to 0.638 μmol m⁻² s⁻¹ bar⁻¹ for a number of species. However, such variability of r_{md} in one leaf as obtained in our experiments raises doubts about how adequately the simple resistance network model describes the CO₂ reassimilation in the mesophyll cells. Nevertheless, the result should be considered as a demonstration of the considerable reassimilation of the photorespiratory CO₂ in the mesophyll cells. Reassimilation almost as efficient as that occurring in steady state occurs during the postillumination burst into CO₂-free air, despite the fact that the RuBP level should rapidly decrease during the burst.

The application of the Rubisco kinetics for the calculation

of carboxylation and oxygenation rates is based on K_{sp} . The value of K_{sp} obtained in this work is in the range of the K_{sp} values of 77 to 88 determined in vitro (Jordan and Ogren, 1981, 1984) but is lower than about 100, the value frequently obtained with leaves (Laisk, 1977; Brooks and Farquhar, 1985; Peterson, 1989). It may be that the method of determining the Γ^* in the presence of dark respiration (Laisk, 1977; Brooks and Farquhar, 1985) leads to underestimation of Γ^* or that the variability of K_{sp} in vivo is real.

None of the lines from the gas-exchange measurements follow the pattern of the CO₂ dependence of photorespiration, $R_p(ETR)$, calculated from fluorescence and Rubisco kinetics in the range of high CO₂ concentrations. $B(CO_2)$ shows the closest trend but is shifted toward more CO₂ uptake. Both $B(0)$ and R_i from the *P*(CO₂) versus *C_c* plot show a continuing CO₂ evolution at high CO₂ concentrations, which cannot be explained by RuBP oxygenation. This CO₂ evolution is not present at low CO₂ concentrations limiting photosynthesis, but appears when photosynthesis becomes CO₂ saturated. It is inhibited neither by high CO₂ nor by low O₂, from which we can conclude that it is not related to the RuBP oxygenase reaction. In parallel with the CO₂ evolution, a CO₂ uptake component is present, which can be seen from the shift of the $B(CO_2)$ curve toward positive values. This CO₂ uptake is not present during photosynthesis at low CO₂ but appears rapidly after light is switched off. It is continuously present during photosynthesis at saturating CO₂. This component of CO₂ uptake explains the difference between *ETR*/4 and *P*(CO₂) at high CO₂ levels, where *ETR* declines with increasing CO₂ faster than *P*(CO₂). Similar extra CO₂ uptake, concomitant with enhanced CO₂ evolution, has been observed at the final phase of the postillumination CO₂ uptake, when PGA concentration had reached its maximum level (Laisk, 1985). It is known that under conditions at which PGA levels are high, considerable export of the PGA to the cytosol and its further metabolism occur (Keerberg et al., 1971). We suggest that carboxylation of PEP and the subsequent decarboxylation of malate and pyruvate (Keerberg et al., 1983) are the dominating non-RuBP carboxylation and decarboxylation during the postillumination period and at high CO₂ levels in the light. The corresponding anaplerotic CO₂ uptake should not be classified as photosynthesis, nor should the corresponding CO₂ evolution be classified as photorespiration.

ACKNOWLEDGMENTS

Cordial thanks to Prof. N.E. Tolbert for discussing and improving the manuscript. The LI-6262 was provided for testing by Dr. D.K. McDermitt (Li-Cor, Lincoln, NE).

Received May 4, 1994; accepted June 16, 1994.

Copyright Clearance Center: 0032-0889/94/106/0689/07.

LITERATURE CITED

- Bravdo BA, Canvin D** (1979) Effect of carbon dioxide on photorespiration. *Plant Physiol* **63**: 399–401
- Brooks A, Farquhar GD** (1985) Effect of temperature on the CO₂/O₂ specificity of ribulose-1,5-bisphosphate carboxylase/oxygenase and the rate of respiration in the light. *Planta* **165**: 397–406
- Brown HT, Escombe ELS** (1900) Static diffusion of gases and liquids in relation to the assimilation of carbon and translocation in plants. *Philos Trans R Soc Lond B Biol Sci* **193**: 223–291

- Cornic G, Briantais J-M** (1991) Partitioning of photosynthetic electron flow between CO₂ and O₂ reduction in a C₃ leaf (*Phaseolus vulgaris* L.) at different CO₂ concentrations and during drought stress. *Planta* **183**: 178–184
- Cowan IR** (1977) Stomatal behaviour and environment. *Adv Bot Res* **4**: 117–228
- Decker JP** (1955) A rapid post-illumination deceleration of respiration in green leaves. *Plant Physiol* **30**: 82–84
- Eichelmann H, Laisk A** (1994) CO₂ uptake and electron transport rates in wild type and starchless mutant of *Nicotiana sylvestris*. The role and regulation of starch synthesis at saturating CO₂ concentrations. *Plant Physiol* **106**: 679–687
- Evans JR, Sharkey TD, Berry JA, Farquhar GD** (1986) Carbon isotope discrimination measured concurrently with gas exchange to investigate CO₂ diffusion in leaves of higher plants. *Aust J Plant Physiol* **13**: 281–292
- Farquhar GD, von Caemmerer S** (1982) Modelling of photosynthetic response to environmental conditions. In OL Lange, PS Nobel, CB Osmond, H Ziegler, eds, *Physiological Plant Ecology*. Encyclopedia of Plant Physiology, New Series, Vol 12B. Springer-Verlag, Berlin, pp 549–588
- Farquhar GD, von Caemmerer S, Berry JA** (1980) A biochemical model of photosynthetic CO₂ assimilation in leaves of C₃ species. *Planta* **149**: 78–90
- Forrester ML, Krotkov G, Nelson CD** (1966) Effect of oxygen on photosynthesis, photorespiration and respiration in detached leaves. I. Soybean. *Plant Physiol* **41**: 422–427
- Genty B, Briantais JM, Baker NR** (1989) The relationship between quantum yield of photosynthetic electron transport and quenching of chlorophyll fluorescence. *Biochim Biophys Acta* **990**: 87–92
- Harley PC, Loreto F, Di Marco G, Sharkey TD** (1992) Theoretical considerations when estimating the mesophyll conductance to CO₂ flux by analysis of the response of photosynthesis to CO₂. *Plant Physiol* **98**: 1429–1436
- Hess JL, Tolbert NE** (1966) Glycolate, glycine, serine and glycerate formation during photosynthesis by tobacco leaves. *J Biol Chem* **241**: 5705–5711
- Jordan DB, Ogren WL** (1981) A sensitive assay procedure for simultaneous determination of ribulose-1,5-bisphosphate carboxylase and oxygenase activities. *Plant Physiol* **67**: 237–245
- Jordan DB, Ogren WL** (1984) The CO₂/O₂ specificity of ribulose 1,5-bisphosphate carboxylase/oxygenase. Dependence on ribulose bisphosphate concentration, pH and temperature. *Planta* **161**: 308–313
- Keerbergh H, Värk E, Keerbergh O, Pärnik T** (1971) The effect of the spectral composition of light on the labelling of amino and organic acids with ¹⁴C during the assimilation of ¹⁴CO₂ by bean leaves. *Proc Acad Sci Estonian SSR Biol* **20**: 350–353 (in Russian)
- Keerbergh O, Keerbergh H, Pärnik T, Viil J, Värk E** (1983) The metabolism of photosynthetically assimilated ¹⁴CO₂ under different concentrations of carbon dioxide. *Int J Appl Radiat Isot* **34**: 861–864
- Kisaki T, Tolbert NE** (1970) Glycine as a substrate for photorespiration. *Plant Cell Physiol* **11**: 247–258
- Laisk A** (1970) A model of leaf photosynthesis and photorespiration. In I Shetlik, ed, *Prediction and Measurement of Photosynthetic Productivity*. Centre for Agricultural Publishing and Documentation, Wageningen, The Netherlands, pp 295–306
- Laisk A** (1977) Kinetics of photosynthesis and photorespiration in C₃ Plants. Nauka Moscow (in Russian)
- Laisk A** (1985) Kinetics of photosynthetic CO₂ uptake in C₃ plants. In J Viil, G Grishina, A Laisk, eds, *Kinetics of Photosynthetic Carbon Metabolism in C₃-Plants*. Valgus, Tallinn, Estonia, pp 21–34
- Laisk A, Kiirats O, Eichelmann H, Oja V** (1987) Gas exchange studies of carboxylation kinetics in intact leaves. In J Biggins, ed, *Progress in Photosynthesis Research*. Martinus Nijhoff Publishers, Dordrecht, The Netherlands, pp 245–252
- Laisk A, Oja V** (1971) A three-channel apparatus for detailed investigation of the leaf CO₂ exchange. In T Frey, ed, *Estonian Contributions to the International Biological Programme*, II. Institute of Zoology and Botany, Academy of Science of Estonian SSR, Tartu, pp 113–128
- Laisk A, Oja V** (1972) A mathematical model of leaf photosynthesis and photorespiration. II. Experimental verification. In AA Nitchiporovitch, ed, *Theoretical Foundations of the Photosynthetic Productivity*. Nauka, Moscow, pp 362–368 (in Russian)
- Laisk A, Oja V, Heber U** (1992) Steady-state and induction kinetics of photosynthetic electron transport related to donor side oxidation and acceptor side reduction of photosystem I in sunflower leaves. *Photosynthetica* **27**: 449–463
- Laisk A, Oja V, Kiirats O** (1984) Assimilatory power (post-illumination CO₂ uptake) in leaves. Measurement, environmental dependencies and kinetic properties. *Plant Physiol* **76**: 723–729
- Lechtenberg D, Voss B, Weis E** (1990) Regulation of photosynthesis: photosynthetic control and thioredoxin-dependent enzyme regulation. In M Baltscheffsky, ed, *Current Research in Photosynthesis*, Vol IV. Kluwer Academic Publishers, Dordrecht, The Netherlands, pp 171–174
- Loreto F, Harley PC, Di Marco G, Sharkey TD** (1992) Estimation of mesophyll conductance to CO₂ flux by three different methods. *Plant Physiol* **98**: 1437–1443
- Lorimer GH** (1981) The carboxylation and oxygenation of ribulose-1,5-bisphosphate: the primary events in photosynthesis and photorespiration. *Annu Rev Plant Physiol* **32**: 349–383
- Ogren WL, Bowes G** (1971) Ribulose diphosphate carboxylase regulates soybean photorespiration. *Nature New Biol* **230**: 159–160
- Oja V, Laisk A, Heber U** (1986) Light-induced alkalization of the chloroplast stroma *in vivo* as estimated from the CO₂ capacity of intact sunflower leaves. *Biochim Biophys Acta* **849**: 355–365
- Oja VM** (1983) A rapid-response gas exchange measuring device for studying the kinetics of leaf photosynthesis. *Fiziol Rast (Sov Plant Physiol)* **30**: 1045–1052
- Pärnik T** (1985) Photorespiratory decarboxylation at different CO₂ concentrations. In J Viil, G Grishina, A Laisk, eds, *Kinetics of Photosynthetic Carbon Metabolism in C₃ Plants*. Valgus, Tallinn, Estonia, pp 121–124
- Peterson RB** (1987) Quantitation of the O₂-dependent, CO₂-reversible component of the postillumination CO₂ exchange transient in tobacco and maize leaves. *Plant Physiol* **84**: 862–867
- Peterson RB** (1989) Partitioning of noncyclic photosynthetic electron transport to O₂ dependent dissipative processes as probed by fluorescence and CO₂ exchange. *Plant Physiol* **90**: 1322–1328
- Sharkey TD** (1988) Estimating the rate of photorespiration in leaves. *Plant Physiol* **73**: 147–152
- Sharkey TD, Vasey TL** (1989) Low oxygen inhibition of photosynthesis is caused by inhibition of starch synthesis. *Plant Physiol* **90**: 385–387
- von Caemmerer S, Evans JR** (1991) Determination of the CO₂ pressure in chloroplasts from leaves of several C₃ plants. *Aust J Plant Physiol* **18**: 287–305
- Weis E, Lechtenberg D** (1989) Fluorescence analysis during steady-state photosynthesis. *Philos Trans R Soc Lond B* **323**: 253–268
- Woo KC, Wong SC** (1983) Inhibition of CO₂ assimilation by supraoptimal CO₂: effect of light and temperature. *Aust J Plant Physiol* **10**: 75–85